

Supporting Information

H₂O₂-Induced Micro-explosion Preparation of Highly-dispersed and Porous MWW Oligolayers and Their properties

Chunna Zhang ^a, Feng Lin ^a, Lingtao Kong ^a, Zhaoqi Ye ^a, Di Pan ^a, Hongbin Li ^a, He Li ^a, Peng Liu ^a, Yahong Zhang ^a, Hongbin Zhang ^{b,*}, and Yi Tang ^{a,*}

^a Department of Chemistry, Laboratory of Advanced Materials, Collaborative Innovation Center of Chemistry for Energy Materials and Shanghai Key Laboratory of Molecular Catalysis and Innovative Materials, Fudan University, Shanghai 200433, China.

^b Institute for Preservation of Chinese Ancient Books, Fudan University Library, Fudan University, Shanghai 200433, China.

* Corresponding author.

Prof. Yi Tang, Email address: yitang@fudan.edu.cn

Dr. Hongbin Zhang, Email address: zhanghongbin@fudan.edu.cn

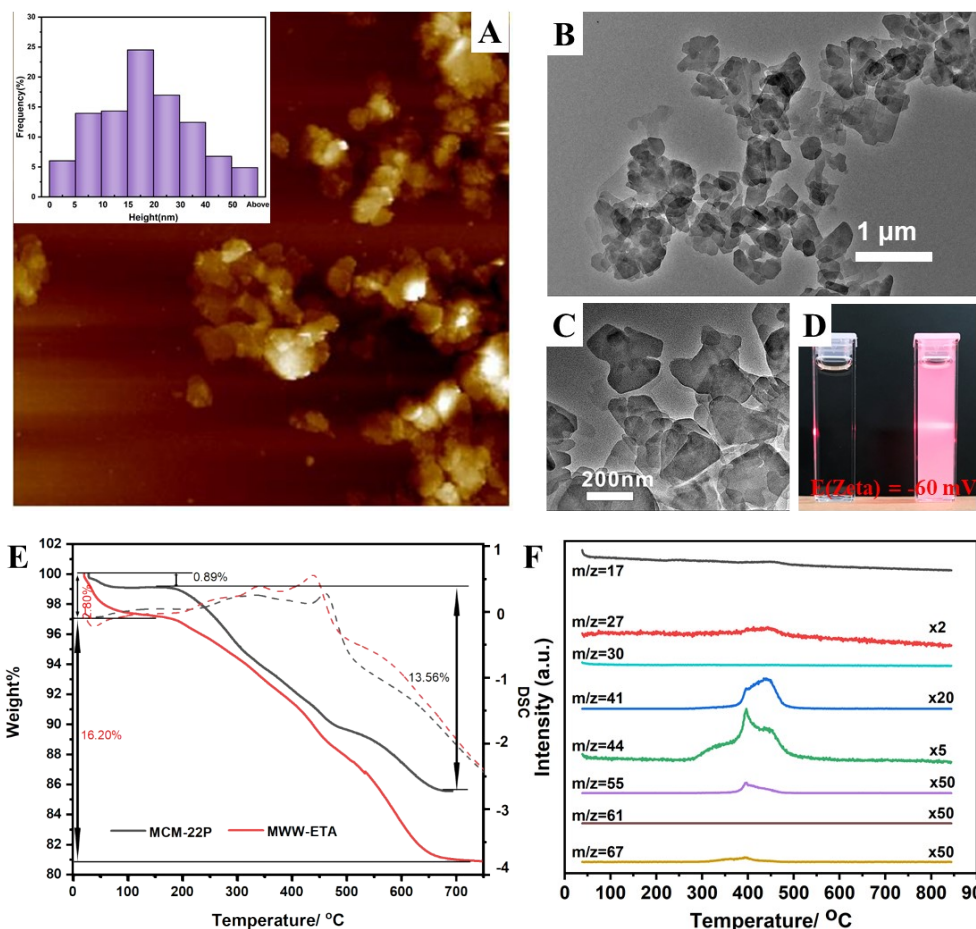


Figure S1. Features of the obtained MWW-ETA. **A**, AFM image shows the average thickness is about 15-20 nm. **B** and **C**, TEM images indicate its discrete, tiled oligolayers. **D**, The obvious Tyndall effect indicates excellent dispersity. **E**, TGA and DSC curves of MCM-22P and MWW-ETA in air. The introduction of ETA leads to an increased weight loss of MWW-ETA. **F**, MS spectra of MWW-ETA. $m/z=17$, 27, 30, 61 are characteristic signals for ETA different from HMI. Both ETA and HMI have a relatively strong interaction with MWW nanosheets.

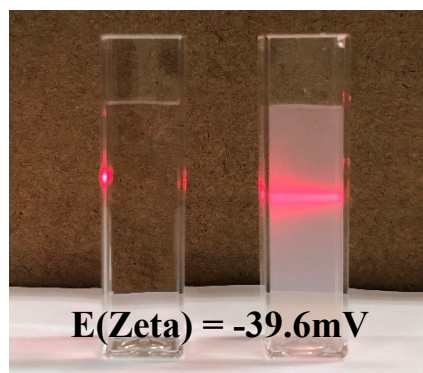


Figure S2. The Tyndall effect and Zeta potential for MWW-ME(4) suspension (Left one: H_2O).

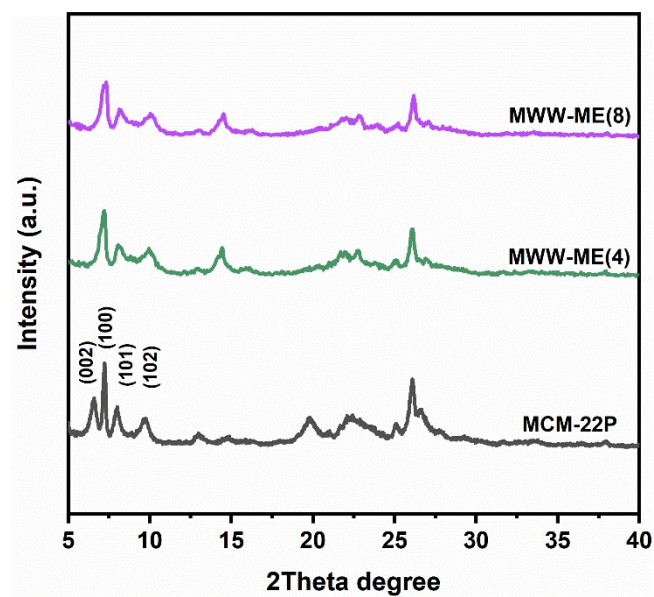


Figure S3. XRD patterns of MCM-22P and MWW-ME(x) samples.

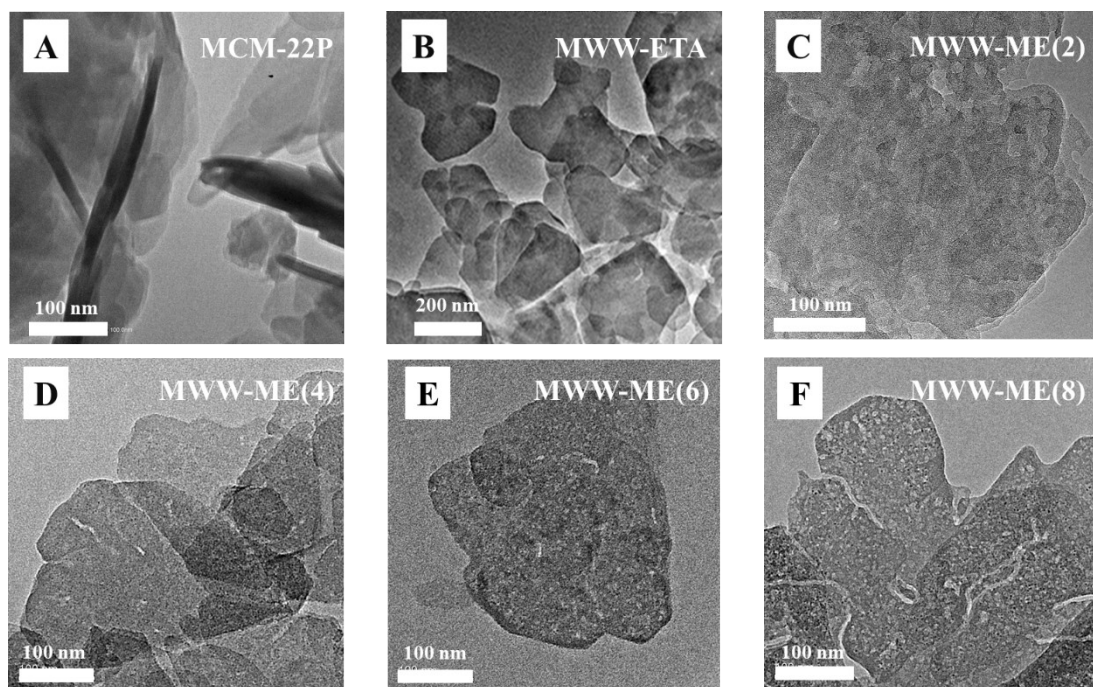


Figure S4. TEM images of MCM-22P (A), MWW-ETA (B), and MWW-ME (C-F) zeolites nanosheets.

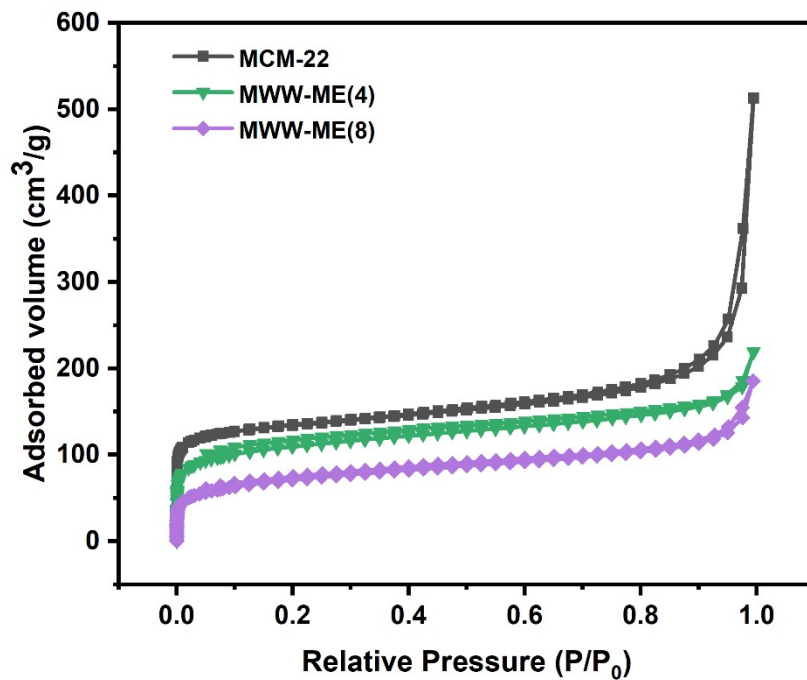


Figure S5. Ar adsorption-desorption isotherms of MCM-22 (gray line) and MWW-ME(x).

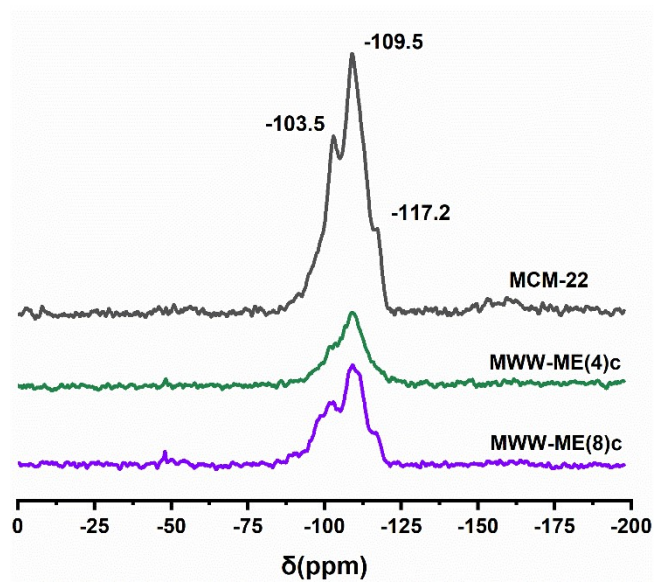


Figure S6. Solid-state ²⁹Si MAS NMR for MCM-22 (gray line) and MWW-ME(x).

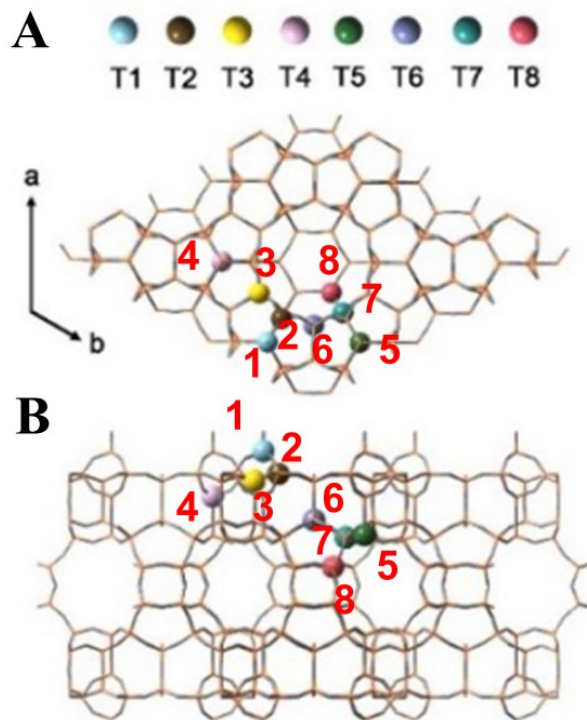


Figure S7. Eight different T sites in MWW framework. (A), along [001]direction. (B), along [100] direction¹.

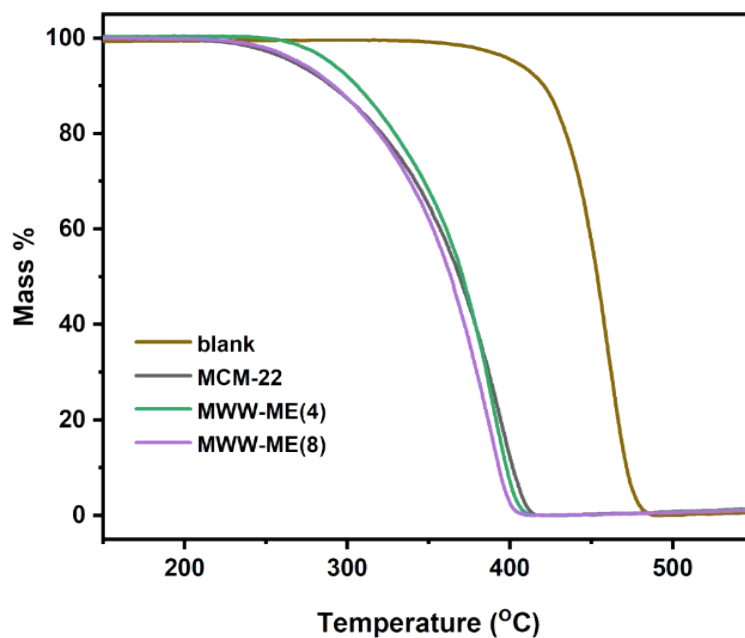


Figure S8. Mass loss curves of PP at temperature program process.

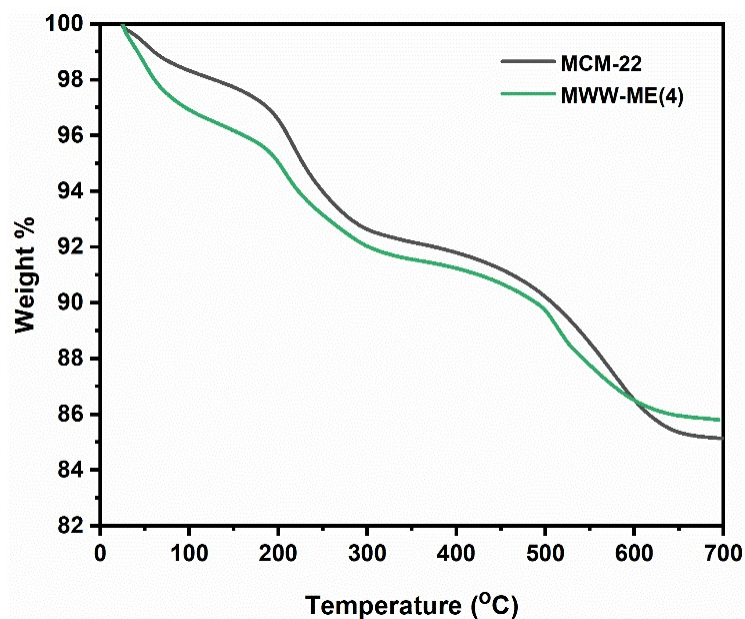


Figure S9. The TG curves of MCM-22 and MWW-ME(4) in the air after the alkylation reaction of mesitylene with benzyl alcohol (BzOH).

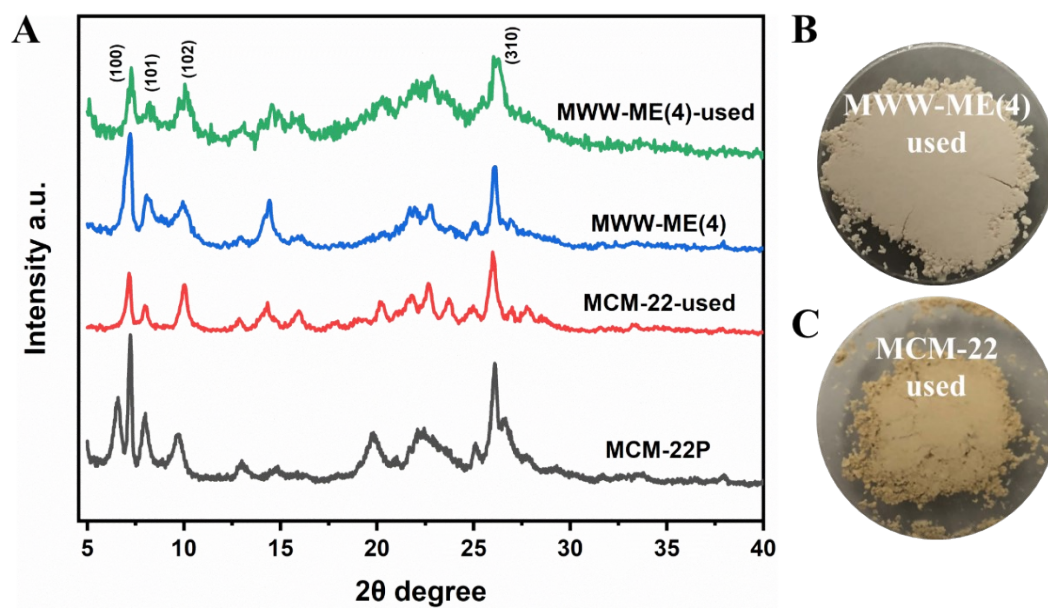


Figure S10. XRD patterns (A) and optical photos of the used MCM-22 (B) and used MWW-ME(4) (C).

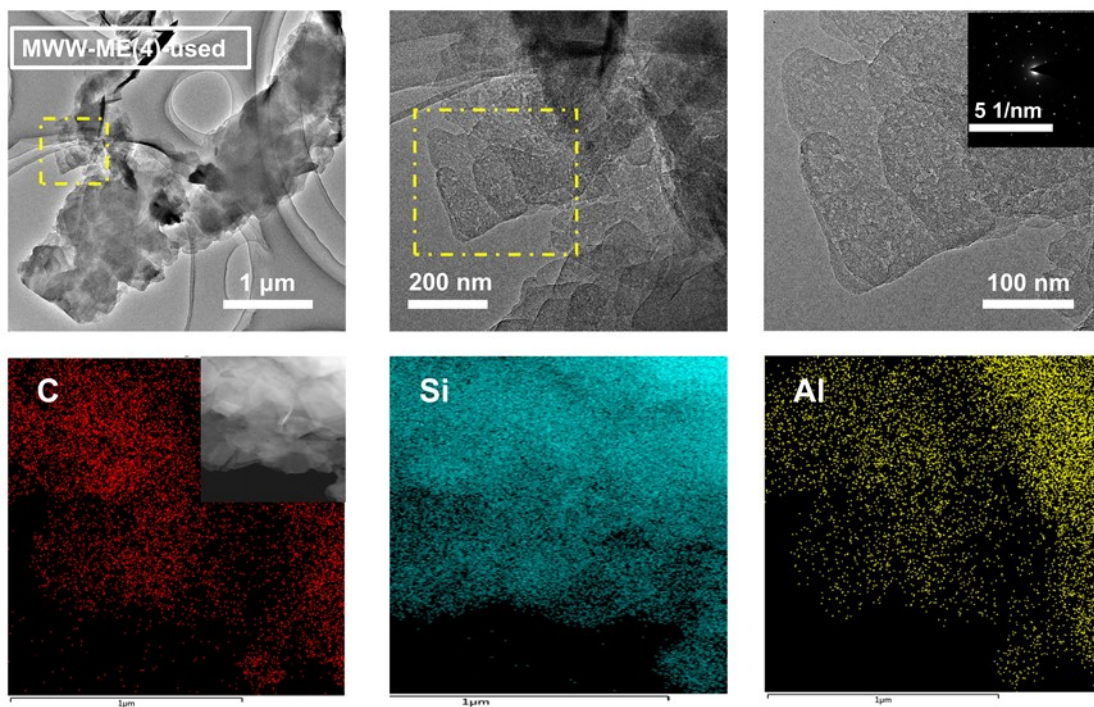


Figure S11. TEM images and EDS Mapping of MWW-ME(4)-used.

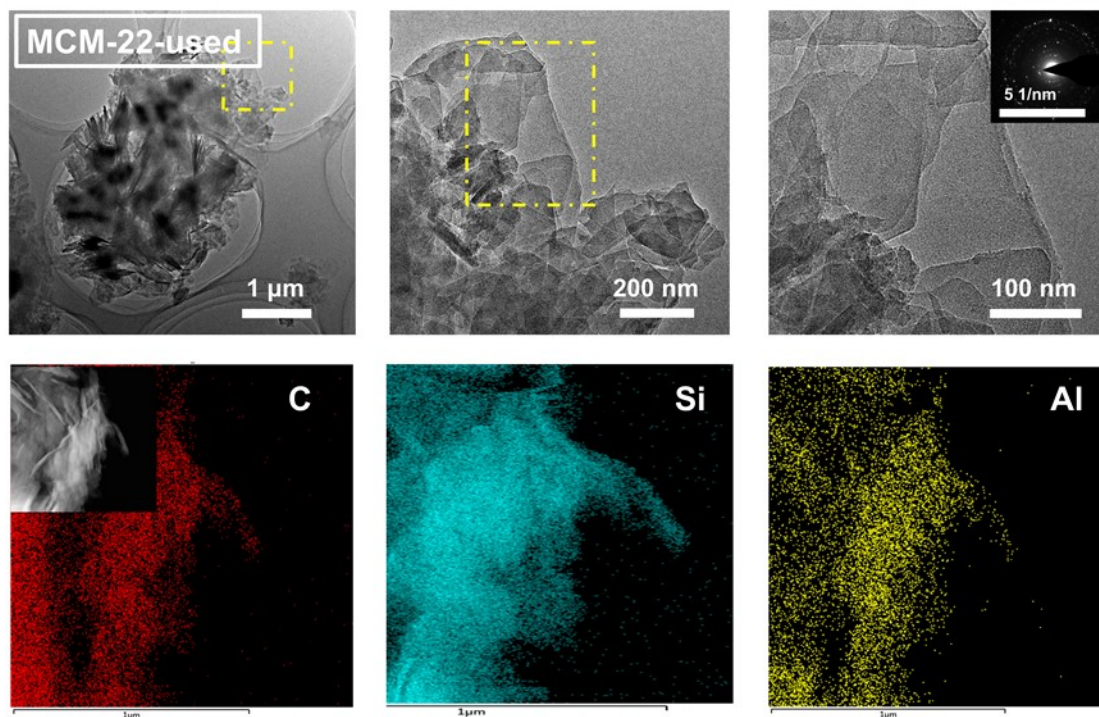


Figure S12. TEM images and EDS Mapping of MCM-22-used.

Table S1. The results of NH₃-TPD tests.

	LT (mmol/g)	HT (mmol/g)	Total (mmol/g)	s/w
MCM-22-ex	0.40	0.28	0.68	0.70
MWW-ME(4)-ex	0.36	0.31	0.67	0.86
MWW-ME(4)	0.41	0.34	0.75	0.83

References

- (1) Zhou, Y.; Mu, Y.; Hsieh, M. F.; Kabius, B.; Pacheco, C.; Bator, C.; Rioux, R. M.; Rimer, J. D. Enhanced Surface Activity of MWW Zeolite Nanosheets Prepared via a One-Step Synthesis. *J Am Chem Soc.* 2020, **142**, 8211-8222.